Self-Assembly and Field-Responsive Optical Diffractions of Superparamagnetic Colloids

ARTICLE *in* LANGMUIR · MAY 2008

Impact Factor: 4.46 · DOI: 10.1021/la7039493 · Source: PubMed

Self-Assembly and Field-Responsive Optical Diffractions of Superparamagnetic Colloids

Jianping Ge, Yongxing Hu, Tierui Zhang, Tuan Huynh, and Yadong Yin*

University of California, Department of Chemistry, Riverside, California 92521

Received December 17, 2007

Ⓦ This paper contains enhanced objects available on the Internet at http://pubs.acs.org/journals/langd5.

Superparamagnetic Fe_3O_4 colloids with highly charged surfaces have been assembled into ordered structures in water in response to external magnetic fields. The colloids form chainlike structures with regular interparticle spacings of a few hundred nanometers along the direction of the external field so that the system strongly diffracts visible light. The balance between attractive (in this case, magnetic) and repulsive (electrostatic) forces dictates interparticle spacing and therefore optical properties. By changing the relative strength of these two forces, one can tune the peak diffraction wavelength over the entire visible spectrum. We were able to optimize the diffraction intensity and the tuning range through studying their dependence on variables such as the size distribution and concentration of the Fe_3O_4 colloids or ionic strength of the solutions. The fast, reversible response and the feasibility for miniaturization impart these photonic materials great potential in applications such as optoelectronic devices, sensors, and color displays.

Introduction

Self-assembly of colloidal particles into periodic arrays has proved to be an effective approach for creating functional photonic materials and devices.[1−5] Monodisperse colloids with submicrometer sizes have been widely used as building blocks to form photonic crystals, that is, crystalline lattices in which a photonic band gap appears as the result of cooperative scattering of light from an ordered array of dielectric particles.[5−15] Driven by potential applications in optical switches, filters, and optical interconnects/circuits, considerable effort has been devoted to the development of tunable photonic crystals whose properties can be controlled by external stimuli. In principle, the stimuli can be any means that effectively change the refractive indices of the colloids or the surrounding matrix, or the lattice constants and symmetry of the colloidal arrays. For example, liquid crystals and oxide materials such as WO_3, VO_2, and $BaTiO_3$ have been used as matrix materials for producing tunable photonic crystals because their refractive indices are sensitive to electric fields or temperature changes.[16−21] The majority of approaches to tunable photonic crystals, however, focus on controlling the lattice constants or spatial symmetry of the crystals through the application of chemical stimuli, mechanical forces, electrical or magnetic fields, or light.[22−30] A notable example is a hydrogel/colloidal array composite in which the lattice spacing can be tuned by the swelling and deswelling of the hydrogel.[1] Polyelectrolyte multilayers have also been used to create tunable structures in silica colloidal crystals by changing the spacing between neighboring spheres through solvent vapor pressure, light, temperature, and electrical actuation.[26,31−33]

Introducing magnetic components to the colloidal building blocks provides an effective means for controlling the interparticle

* To whom correspondence should be addressed. E-mail: yadong.yin@ucr.edu.

(1) Holtz, J. H.; Asher, S. A. *Nature* **1997**, *389*, 829−832.
(2) Blanco, A.; Chomski, E.; Grabtchak, S.; Ibisate, M.; John, S.; Leonard, S. W.; Lopez, C.; Meseguer, F.; Miguez, H.; Mondia, J. P.; Ozin, G. A.; Toader, O.; van Driel, H. M. *Nature* **2000**, *405*, 437−440.
(3) Velev, O. D.; Lenhoff, A. M.; Kaler, E. W. *Science* **2000**, *287*, 2240−2243.
(4) Jiang, P.; Ostojic, G. N.; Narat, R.; Mittleman, D. M.; Colvin, V. L. *Adv. Mater.* **2001**, *13*, 389−393.
(5) Schroden, R. C.; Al-Daous, M.; Blanford, C. F.; Stein, A. *Chem. Mater.* **2002**, *14*, 3305−3315.
(6) Xia, Y.; Gates, B.; Yin, Y.; Lu, Y. *Adv. Mater.* **2000**, *12*, 693−713.
(7) López, C. *J. Opt. A: Pure Appl. Opt.* **2006**, *8*, R1−R14.
(8) Halaoui, L. I.; Abrams, N. M.; Mallouk, T. E. *J. Phys. Chem. B* **2005**, *109*, 6334−6342.
(9) Van Blaaderen, A. *MRS Bull.* **1998**, *23*, 39−43.
(10) Hillebrand, R.; Gösele, U. *Science* **2004**, *305*, 187−188.
(11) Prasad, T.; Mittleman, D. M.; Colvin, V. L. *Opt. Mater.* **2006**, *29*, 56−59.
(12) Asher, S. A.; Sharma, A. C.; Goponenko, A. V.; Ward, M. M. *Anal. Chem.* **2003**, *75*, 1676−1683.
(13) Goponenko, A. V.; Asher, S. A. *J. Am. Chem. Soc.* **2005**, *127*, 10753−10759.
(14) Braun, P. V.; Rinne, S. A.; García-Santamaría, F. *Adv. Mater.* **2006**, *18*, 2665−2678.
(15) Lawrence, J. R.; Ying, Y.; Jiang, P.; Foulger, S. H. *Adv. Mater.* **2006**, *18*, 300−303.
(16) Kuai, S.-L.; Bader, G.; Ashrit, P. V. *Appl. Phys. Lett.* **2005**, *86*, 221110.
(17) Pevtsov, A. B.; Kurdyukov, D. A.; Golubev, V. G.; Akimov, A. V.; Meluchev, A. A.; Sel'kin, A. V.; Kaplyanskii, A. A.; Yakovlev, D. R.; Bayer, M. *Phys. Rev. B* **2007**, *75*, 153101.
(18) Ji, Z.; Sun, C. Q.; Pita, K.; Lam, Y. L.; Zhou, Y.; Ng, S. L.; Kam, C. H.; Li, L. T.; Gui, Z. L. *Appl. Phys. Lett.* **2001**, *78*, 661−663.
(19) Kang, D.; Maclennan, J. E.; Clark, N. A.; Zakhidov, A. A.; Baughman, R. H. *Phys. Rev. Lett.* **2001**, *86*, 4052−4055.
(20) Leonard, S. W.; Mondia, J. P.; van Driel, H. M.; Toader, O.; John, S.; Busch, K.; Birner, A.; Gösele, U.; Lehmann, V. *Phys. Rev. B* **2000**, *61*, R2389−R2392.
(21) Mach, P.; Wiltzius, P.; Megens, M.; Weitz, D. A.; Lin, K.-H.; Lubensky, T. C.; Yodh, A. G. *J. Europhys. Lett.* **2002**, *58*, 679−685.
(22) Barry, R. A.; Wiltzius, P. *Langmuir* **2006**, *22*, 1369−1374.
(23) Gu, Z. Z.; Fujishima, A.; Sato, O. *J. Am. Chem. Soc.* **2000**, *122*, 12387−12388.
(24) Sumioka, K.; Kayashima, H.; Tsutsui, T. *Adv. Mater.* **2002**, *14*, 1284−1286.
(25) Jeong, U.; Xia, Y. *Angew. Chem., Int. Ed.* **2005**, *44*, 3099−3103.
(26) Fleischhaker, F.; Arsenault, A. C.; Kitaev, V.; Peiris, F. C.; von Freymann, G.; Manners, I.; Zentel, R.; Ozin, G. A. *J. Am. Chem. Soc.* **2005**, *127*, 9318−9319.
(27) Lumsdon, S. O.; Kaler, E. W.; Williams, J. P.; Velev, O. D. *Appl. Phys. Lett.* **2003**, *82*, 949−951.
(28) Xia, J.; Ying, Y.; Foulger, S. H. *Adv. Mater.* **2005**, *17*, 2463−2467.
(29) Kamenjicki Maurer, M.; Lednev, I. K.; Asher, S. A. *Adv. Funct. Mater.* **2005**, *15*, 1401−1406.
(30) Snoswell, D. R. E.; Bower, C. L.; Ivanov, P.; Cryan, M. J.; Rarity, J. G.; Vincent, B. *New J. Phys.* **2006**, *11*, 267.
(31) Tétreault, N.; Arsenault, A. C.; Mihi, A.; Wong, S.; Kitaev, V.; Manners, I.; Miguez, H.; Ozin, G. A. *Adv. Mater.* **2005**, *17*, 1912−1916.
(32) Fleischhaker, F.; Arsenault, A. C.; Wang, Z.; Kitaev, V.; Peiris, F. C.; von Freymann, G.; Manners, I.; Zentel, R.; Ozin, G. A. *Adv. Mater.* **2005**, *17*, 2455−2458.
(33) Arsenault, A. C.; Puzzo, D. P.; Manners, I.; Ozin, G. A. *Nat. Photon.* **2007**, *1*, 468−472.

10.1021/la7039493 CCC: $40.75
Published on Web 02/13/2008

spacing and thus the photonic properties of colloidal assemblies. The choice of magnetic fields as the external stimulus may offer improved spectral tunability, response rate, and facility of integration into existing photonic systems. The main challenge along this path lies in the production of magnetic colloidal building blocks with controllable size, morphology, stability, surface structure, and magnetic properties. The pioneer work by Asher et al. focused on polymer colloids embedded with superparamagnetic nanoparticles of iron oxide.[34−36] Although field-responsive diffraction with a considerable tuning range was realized, the volume fraction of the magnetically active materials was limited, suggesting that great improvement upon the overall performance of magnetically tuned photonic materials could be realized through increased loading of magnetic materials. It has also been shown that emulsion droplets containing iron oxide nanoparticles organize into ordered structures in the presence of an external magnetic field.[37,38] Since emulsions are not thermodynamically stable systems, the long-term stability of the oil droplets against dissociation or aggregation is questionable. Ideally, pure magnetic materials can be made into colloidal forms to significantly increase the magnetic moment of each particle.[39] However, a superparamagnetic-to-ferromagnetic transition commonly occurs as particles are grown into larger domains, causing irreversible aggregation of particles upon magnetization. An alternative approach is to form colloidal clusters or aggregates of superparamagnetic nanocrystals to increase the magnetization in a controllable manner while retaining the superparamagnetic characteristics, for example, through controlled evaporation of the low-boiling point oil phase from microemulsion droplets that contain presynthesized nanocrystals.[40]

We have recently developed a high-temperature solution-phase process for the synthesis of superparamagnetic colloidal nanocrystal clusters (CNCs; uniform three-dimensional aggregates of magnetite (Fe_3O_4) nanocrystals).[41] Each cluster is composed of many interconnected Fe_3O_4 nanocrystals with sizes of ∼10 nanometers so that they display superparamagnetism despite the large, magnetically active volume of each cluster. Because of their highly charged polyacrylate capped surfaces and the large magnetic moment per cluster, these colloids form ordered structures and display tunable diffractions in the presence of external magnetic fields.[42] In comparison to previously reported iron oxide/polymer composite colloids (17.0 wt % γ-Fe_2O_3),[34−36] the magnetite CNCs are composed of pure iron oxide and thus have a much greater magnetic moment per particle and higher refractive index. Because of their strong magnetic responses, the CNC particles can be quickly (less than 1 s) assembled into ordered structures directly from a relatively diluted dispersion, while in the polymer composite case the external magnetic field was only able to deform the preformed colloidal crystals. Consequently, the strength of the external magnetic field required to induce changes in diffraction is also much lower in the current case (100−400 Oe vs 2.7 KOe). This system also has the advantage of wide tunability in diffraction wavelength (∼400−800 nm), which has not been previously achieved using magnetic stimuli. The high refractive index of magnetite CNCs makes it possible to obtain a relatively high diffraction intensity even with a small volume fraction of particles (∼0.055%), while in the case of polymer composite colloids a high volume fraction (>4.2%) is needed to form ordered crystals.

In this paper, we report our extended studies of the assembly behavior of the colloidal CNC particles, and the roles that electrostatic and induced magnetic forces play in determining their assembled structures and photonic properties. This article is more than a simple extension of the results that we have published previously. We provide here convincible experimental observations which allow us to clarify the self-assembly behavior of the magnetic particles and the origin of the diffractions. The optical response of the system can now be tuned independently by changing the electrostatic or magnetic interactions between the CNC particles. The tuning range of the system can be further extended by mixing particles with multiple average sizes. The position and intensity of diffraction peaks and the tuning range of the system can be optimized according to the size, size distribution, and concentration of the magnetic particles, and the ionic strength of the solution. In addition, we demonstrate that this system allows for convenient miniaturization while maintaining optical responses to the external field, which may lead to practical applications in many integrated photonic devices.

Experimental Section

Materials. Diethylene glycol (DEG, reagent grade), ethanol (denatured), and sodium hydroxide (NaOH, 98.8%) were purchased from Fisher Scientific. Anhydrous iron(III) chloride ($FeCl_3$, 98%) was purchased from Riedel-de Haën. Poly(acrylic acid) (PAA, MW = 1800) was obtained from Sigma-Aldrich. All chemicals were directly used as received without further treatment.

Synthesis of Superparamagnetic Fe_3O_4 CNCs. Magnetite colloidal nanocrystal clusters (CNCs) with a tunable average size in the range from ∼30 to ∼180 nm were synthesized in solution at high temperature.[41] A NaOH/DEG stock solution was prepared by dissolving 50 mmol of NaOH in 20 mL of DEG and then heating it at 120 °C for 1 h under nitrogen. In a typical synthesis, a mixture of 4 mmol of PAA, 0.4 mmol of $FeCl_3$, and 17 mL of DEG was heated to 220 °C in a nitrogen atmosphere for 30−60 min with vigorous stirring to form a transparent, light yellow solution. A total of 1.75 mL of NaOH/DEG stock solution was then injected into the above solution which slowly turned black after about 2 min. The resulting mixture was further heated for 1 h to yield about 90 nm Fe_3O_4 CNCs. These colloids were first washed with a mixture of deionized (DI) water and ethanol and then with pure water several times, and finally dispersed in 3 mL of DI water.

Characterization of Fe_3O_4 CNCs. A Tecnai T12 transmission electron microscope (TEM) was used to characterize the morphology and size distribution of the Fe_3O_4 CNCs. Colloids dispersed in water at an appropriate concentration were cast onto a carbon-coated copper grid, followed by evaporation under vacuum at room temperature. A Zeiss AXIO Imager optical microscope was used to observe the visible-range diffraction by CNC solutions enclosed in glass capillaries and the assembly of Fe_3O_4 CNCs under a magnetic field.

Diffraction Measurements. The diffraction spectra of the photonic crystals were measured by using an Ocean Optics HR2000CG-UV-NIR spectrometer coupled to a six-around-one reflection/backscattering probe. Incident light emerges from six fibers, and the light back-diffracted by the colloidal crystals is collected by a central fiber. In a typical measurement, a thin glass vessel containing the solution of F_3O_4 CNCs was placed between the NdFeB magnet and reflection probe. The probe was perpendicular to the glass vessel and parallel to the direction of the magnetic field. Reflection peaks

(34) Xu, X.; Friedman, G.; Humfeld, K. D.; Majetich, S. A.; Asher, S. A. *Adv. Mater.* **2001**, *13*, 1681−1684.
(35) Xu, X.; Friedman, G.; Humfeld, K. D.; Majetich, S. A.; Asher, S. A. *Chem. Mater.* **2002**, *14*, 1249−1256.
(36) Sacanna, S.; Philipse, A. P. *Langmuir* **2006**, *22*, 10209−10216.
(37) Bibette, J. *J. Magn. Magn. Mater.* **1993**, *122*, 37−41.
(38) Calderon, F. L.; Stora, T.; Mondain Monval, O.; Poulin, P.; Bibette, J. *Phys. Rev. Lett.* **1994**, *72*, 2959−2962.
(39) Deng, H.; Li, X. L.; Peng, Q.; Wang, X.; Chen, J. P.; Li, Y. D. *Angew. Chem., Int. Ed.* **2005**, *44*, 2782−2785.
(40) Bai, F.; Wang, D.; Huo, Z.; Chen, W.; Liu, L.; Liang, X.; Chen, C.; Wang, X.; Peng, Q.; Li, Y. *Angew. Chem., Int. Ed.* **2007**, *46*, 6650−6653.
(41) Ge, J.; Hu, Y.; Biasini, M.; Beyermann, W. P.; Yin, Y. *Angew. Chem., Int. Ed.* **2007**, *46*, 4342−4345.
(42) Ge, J.; Hu, Y.; Yin, Y. *Angew. Chem., Int. Ed.* **2007**, *46*, 7428−7431.

were measured with the magnet fixed at a certain distance from the samples. For measuring the diffraction of photonic crystals in modulated magnetic fields, a tubular electromagnet (Magnetic Sensor Systems, E-20-100-27) controlled by a function generator was used to produce periodical magnetic fields. The spectra integration time of collecting the signals was set to be 500 ms for constant magnetic fields and 200 or 100 ms for modulated magnetic fields.

In Situ Observation of the Assembly of Fe_3O_4 CNCs. A 5 μL Fe_3O_4 CNC solution was sandwiched between two thin 3/4″ × 3/4″ cover glass slides to form a thin liquid film and then transferred onto the stage of an optical microscope for in situ observation. A NdFeB magnet was placed on another stage beneath the sample stage and could be manually moved vertically to change the magnet−sample distance.

Results and Discussion

Water soluble magnetite CNCs were produced through a high-temperature hydrolysis reaction of $FeCl_3$ with NaOH in the presence of PAA.[41] The solvent, DEG, partially reduces trivalent iron at the reaction temperature (220 °C) and finally produces Fe_3O_4 particles through dehydration.[39,43,44] Depending on the relative ratios of reagents, this system allows the production of single crystalline nanodots and polycrystalline flowerlike three-dimensional clusters.[41,45] Under optimized conditions, uniform CNCs with average diameters tunable from ∼30 to ∼180 nm are routinely produced. Each CNC is composed of small primary nanocrystals of ∼10 nm, thus retaining superparamagnetism at room temperature while showing much higher saturation magnetization than individual nanodots. Polyacrylate binds to the particle surface through the strong coordination of carboxylate groups with iron cations. The uncoordinated carboxylate groups on the polymer chains extend into the aqueous solution, rendering the particle surfaces highly charged. After removing excess surfactant through repeated cleaning by centrifugation, the CNCs form a stable aqueous dispersion. The PAA coating confers excellent stability against aggregation upon the particles. For example, the particles can be separated from the solution and dried at 60 °C overnight. After storing in powder form for several months, they can still be dispersed instantly in water without detectable aggregation.

Solutions of the Fe_3O_4 CNCs show brilliant colors when an external magnetic field is applied, indicating the formation of ordered structures.[42] This effect, observable in the direction parallel to the external field, results from Bragg diffraction of ambient light by the periodically ordered structures self-assembled from CNCs under the magnetic field.[37,38] The diffraction wavelength can be tuned from longer to shorter values by simply increasing the magnetic field strength. A magnetic field with a strength above 100 G is sufficient to induce the ordering of CNCs and the color change in a bulk solution enclosed in a glass vial. This system also allows for convenient miniaturization while maintaining an optical response to the external field. We have demonstrated this advantage by simply placing a 120 nm Fe_3O_4 CNC solution into a glass capillary with an inner diameter of ∼265 μm. As shown in the optical microscopy images in Figure 1, a magnet placed beneath the capillary drives the color change progressing from red to yellow, green, and blue by simply changing the magnet−capillary distance. The optical response of the small volume sample to the external field is rapid and reversible, demonstrating the feasibility of miniaturization of the system for integration into optoelectronic devices.

(43) Fievet, F.; Lagier, J. P.; Figlarz, M. *MRS Bull.* **1989**, *14*, 29−34.
(44) Sun, Y.; Mayers, B.; Herricks, T.; Xia, Y. *Nano Lett.* **2003**, *3*, 955−960.
(45) Ge, J.; Hu, Y.; Biasini, M.; Dong, C.; Guo, J.; Beyermann, W. P.; Yin, Y. *Chem.—Eur. J.* **2007**, *13*, 7153−7161.

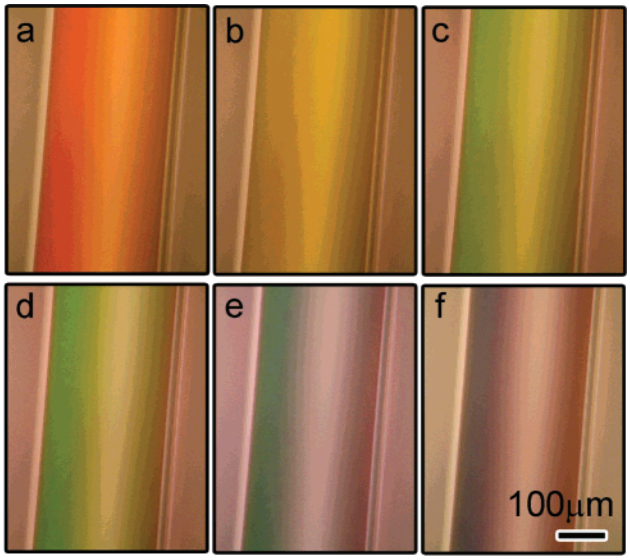

Figure 1. Optical microscope images of a 120 nm Fe_3O_4 CNC solution enclosed in a glass capillary under an increasing (from a to f) magnetic field.

Self-Assembly of CNCs in External Magnetic Fields. The self-assembly behavior of the CNCs in response to external magnetic fields has been studied in situ through optical microscopy. A thin film of CNC solution is formed by sandwiching a CNC droplet between two cover glasses, and then mounted on the sample stage of the microscope. A magnet is placed on another stage underneath the sample so that the magnet can be moved vertically for convenient control of the sample−magnet distance. Without an external magnetic field, the superparamagnetic colloids are well dispersed in water and their Brownian motion makes it difficult to capture a clear image of the particles. When a magnetic field is vertically applied and gradually strengthened, the movement of particles slows down. At first sight, the increased magnetic field appears to induce a decrease of the particle number density, as can be seen by comparing the dark-field optical microscopy images in Figure 2a and b. A careful inspection also indicates short-range hexagonal order of the particle assembly (Figure 2b). A slight tilt (∼15°) of the magnet reveals that each bright spot is, in fact, a chain of particles lined up along the magnetic field (Figure 2c). The chains appear longer when the magnetic field is tilted further away from vertical orientation. The formation of chains along the magnetic field explains why the particle number density seemingly decreases upon application of the field. We also observed that the separation between the chains (∼2 μm) does not change significantly upon further increase of the magnetic field beyond the value necessary for hexagonal ordering to emerge.

The strong optical diffraction is believed to result from periodicity formed along the magnetic field. In the plane perpendicular to the magnetic field, the short-range order and the large interparticle distance of the assembled structure make it unlikely to diffract visible light. Only in the direction of the external field, chainlike structures form with an interparticle distance (periodicity) comparable to the wavelength of visible light. As schematically shown in Figure 3a, the Fe_3O_4 colloidal crystal is highly anisotropic in structure so that it appears more like arrays of parallel CNC chains. The structural anisotropy also leads to the anisotropic optical responses. Figure 3b and c shows the optical response of a sample confined in a rectangular cuvette when observed parallel and perpendicular to the magnetic field, respectively. A strong visible Bragg diffraction can be

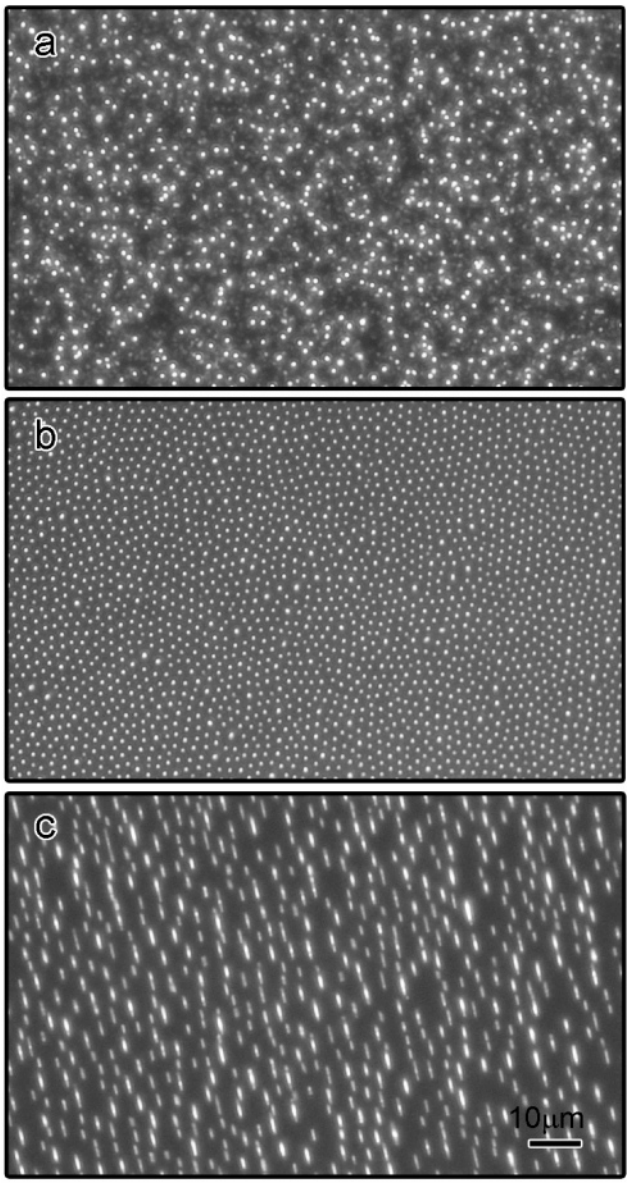

Figure 2. (a and b) Optical microscope images showing the assembly of Fe_3O_4 CNCs dispersed in a liquid film encapsulated between two glass slides in a magnetic field parallel to the viewing angle. The field strength increases from (a) to (b). (c) Optical microscope image illustrating the assembly of CNCs into chainlike structures by slight tilting of the magnetic field (~15° from the view angle).

noticed when observed in the direction parallel to the magnetic field, while only a golden luster can be captured in the perpendicular direction.

When highly charged superparamagnetic colloids are assembled in an external magnetic field, the final ordered structure is the balanced result of both electrostatic interactions and induced magnetic forces.[35] In the absence of a magnetic field, the Fe_3O_4 CNCs disperse well in water at a typical concentration of 8.4 mg/mL. At this concentration, the average interparticle distance is apparently large so that no strong electrostatic repulsive interaction is present to drive the self-assembly of CNCs into ordered arrays. This is different from the previously reported case of magnetically tunable colloidal crystals where charged superparamagnetic polystyrene spheres are highly concentrated so that the strong electrostatic repulsive forces drive the self-assembly of the particles into ordered structures even without an external magnetic field.[35] In the current work, the electrostatic

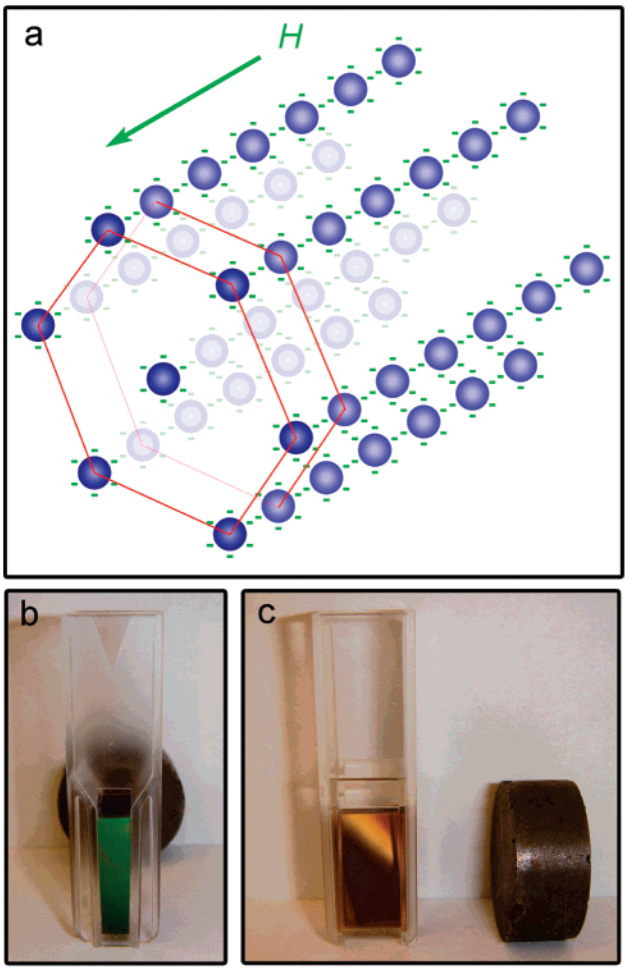

Figure 3. (a) Schematic illustration of the structure of Fe_3O_4 colloids self-assembled in the presence of an external magnetic field. (b and c) Digital photos of a CNC solution captured from the direction (b) parallel and (c) perpendicular to the magnetic field.

interactions do not contribute to the ordering of the CNCs until the magnetic field is applied.

The application of a magnetic field to superparamagnetic colloids in solution results in additional magnetic packing forces and magnetic dipole−dipole interactions.[46,47] The magnetic packing force $F_m = \nabla(\mu B)$, with μ being the induced magnetic moment and B being the strength of the external field, is exerted on every particle and attracts them toward the maximum of local magnetic gradient.[35] The magnetic dipolar interactions can be either attractive or repulsive, strongly depending on the relative orientation of the two magnetic moments. Considering in the current case where the induced magnetic dipoles are parallel to the magnetic field, a magnetic attractive force $F_{ma} = 6(\mu^2/d^4)$ exists when two identical interacting dipoles are aligned with their connecting line parallel to the direction of the magnetic field, while a repulsive force $F_{mr} = 3(\mu^2/d^4)$ presents when the two dipoles are positioned with their connecting line perpendicular to the field (d is the spacing between the two magnetic dipoles). Our estimation shows that the magnetic packing force is relatively small in comparison to the magnetic attractive force. For example, a 120 nm cluster shows a magnetic moment μ of $\sim 6.3 \times 10^{-14}$ emu in a 235 G magnetic field and experiences a magnetic packing force of 1.3×10^{-11} dyn in a gradient of 200 G/cm. With a 197.4

(46) Chabay, R. W.; Sherwood, B. A. *Electric and Magnetic Interactions*; Wiley: New York, 1995; p 672.
(47) Kraftmakher, Y. *Eur. J. Phys.* **2007**, *28*, 409−414.

nm nearest-neighbor spacing d derived from the diffraction peak position, the interparticle attractive force $F_{ma} = 6(\mu^2/d^4)$ is estimated to be 1.6×10^{-7} dyn. Therefore, the magnetic attractive force is believed to play a dominant role in bringing CNCs together.

The electrostatic repulsive force (F_{er}) for the same sample in a 235 G field with a 197.4 nm interparticle spacing is also calculated and compared to the induced magnetic forces. The unbounded carboxylate groups on the particle surface were first converted to the acid form using slightly excessive diluted HCl. The amount of free carboxylate groups was estimated by matching the pH of a pure PAA solution to that of the sample. The ionic strength (I) of the solution is thus estimated to be 3.4×10^{-4} mol/L. The Debye−Hückel length κ^{-1} was calculated to be 16.56 nm according to its definition $\kappa^{-1} = (\epsilon kT/2000N_A e^2 I)^{1/2}$, where ϵ is the dielectric constant, k is Boltzmann's constant, T is the absolute temperature in kelvins, N_A is Avogadro's number, and e is the elementary charge.[48] The zeta potential (ζ) was measured to be −51 mV. Since the 120 nm cluster shows a magnetic moment μ of $\sim 6.3 \times 10^{-14}$ emu in a 235 G magnetic field and a 197.4 nm spacing d can be derived from the diffraction peak, the particle diameter (r) and interparticle surface-to-surface distance (h) are 60 and 77.4 nm, respectively. Using the formula $F_{er} = \pi\epsilon\zeta^2\kappa r e^{-\kappa h}$, the electrostatic repulsive force is calculated to be 2.4×10^{-7} dyn, which is comparable to the estimated magnetic attractive force.

When the electrostatic repulsive force and magnetic attractive force reach a balance, the CNCs form chainlike structures along the external magnetic field with regular interparticle spacing of a few hundred nanometers. The repulsive forces, both electrostatic and magnetic, keep the CNC chains away from each other so that they may self-organize into short-range ordered structures.

Tuning the Diffraction Wavelength by Varying the External Magnetic Field Strength. The spacing between neighboring CNCs within each chain can be changed by varying the strength of external magnetic fields. By moving a magnet closer to the sample, one can conveniently increase the strength of the field and therefore the induced magnetic attractive force, in turn bringing CNC particles closer together until the magnetic attractive force is balanced by the increased interparticle electrostatic repulsion.

Figure 4a shows the reflection spectra of an aqueous solution of 108 nm CNCs (~8.4 mg/mL) in response to a varying magnetic field achieved by controlling the distance between a NdFeB magnet and the sample. By moving the magnet closer to the sample from 3.2 to 1.8 cm, the local magnetic field increases from 125 to 440 G and the diffraction peak shifts from 676 to 412 nm. The spatial dependence of the magnetic field strength of the NdFeB magnet used in this work is displayed in Figure 4b. By using Bragg's law $\lambda = 2nd \sin\theta$, where λ is the diffraction wavelength, n is the refractive index of water, d is the lattice plane spacing, and $\theta = 90°$ is the Bragg angle, we are able to estimate the interparticle spacing within a single chain.[35] As a result, the reflection spectra in Figure 4a can be replotted in Figure 4c, showing a very clear trend for the dependence of the interparticle spacing on the strength of the magnetic field. Changes in the reflection spectra due to repositioning of the magnet are reversible, with the diffraction peak intensity and position being well reproduced at a fixed sample−magnet distance.

Tuning the Diffraction Wavelength by Electrostatic Interactions. Electrostatic interactions also contribute significantly to the assembly of CNC particles. In principle, in a magnetic field with fixed strength, any changes leading to stronger electrostatic repulsion between CNCs will increase the interparticle distance, therefore red-shifting the diffraction peak. When a stronger magnetic field is applied to balance the increased electrostatic repulsion, the CNCs are organized with improved long-range order so that the diffraction intensity increases. These intuitive considerations have been observed experimentally. Immediately following synthesis, the system contains a large amount of free sodium polyacrylate and other ions, which effectively screen the electrostatic repulsive interactions. Only after prewashing with mixtures of ethanol and DI water does the colloidal aqueous solution display diffraction under a magnetic field. Furthermore, the overall diffraction intensities increase significantly after additional cycles of cleaning. Figure 5 shows the variation of magnetically induced reflection spectra of a 130

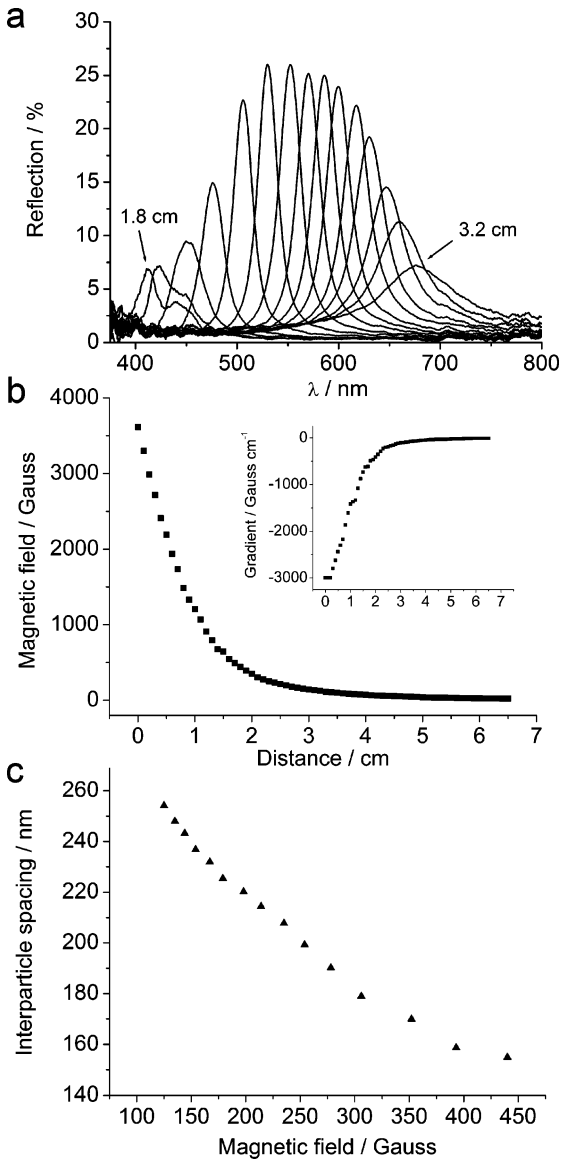

Figure 4. (a) Reflection spectra of a 108 nm CNC solution in response to an external magnetic field with varying strength achieved by changing the magnet−sample distance. The diffraction peak blue-shifts as the distance decreases from 3.2 to 1.8 cm with step size of 0.1 cm. (b) Spatial distribution of the magnetic field strength and gradient (inset) measured using a Hall probe. (c) Relation between the estimated interparticle spacing along the magnetic field and the strength of the magnetic field.

Ⓦ A video showing the field-responsive optical diffractions of the CNC solution in a glass vial is available in mpg format.

(48) Myers, D. *Surfaces, Interfaces, and Colloids: Principles and Applications*, 2nd ed.; Wiley VCH: New York, 1999.

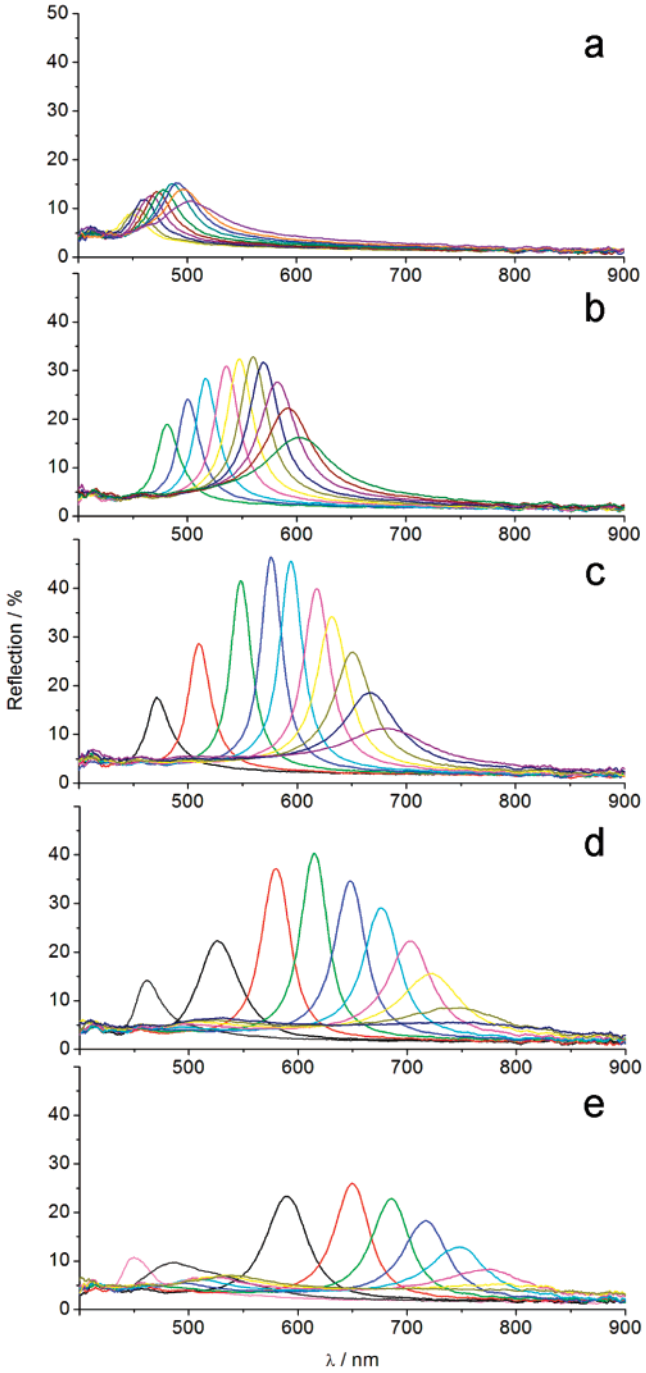

Figure 5. Reflection spectra of a 130 nm CNC solution after additional washing cycles (1−5 for a−e, respectively) with pure DI water. The starting sample was precleaned with a mixture of ethanol and water to remove most of the solvent and extra surfactants. Diffraction peaks blue-shift as the magnet−sample distance decreases from (a) 3.5 to 2.6 cm, (b) 3.1 to 2.2 cm, (c) 2.9 to 2.0 cm, (d) 2.8 to 1.9 cm, and (e) 2.7 to 1.8 cm. Peaks obtained at a specific distance were plotted in the same color.

nm CNC solution with the number of additional washing cycles (1−5 for a−e, respectively). The diffraction spectra obtained at a certain magnet−sample distance in different washing cycles are plotted in the same color. At a fixed magnetic strength, the diffraction peaks consistently red-shift with an increased number of washing cycles, indicating the increase of repulsive electrostatic interactions as more stray electrolytes are removed from the solution.[49,50] With increasing numbers of washing cycles, stronger magnetic fields (or shorter sample−magnet distances) are required to keep the CNC solution diffractive at a given wavelength. Since the magnetic attractive force, $F_{ma} = 6(\mu^2/d^4)$, scales with the square of the induced magnetic moment, a higher magnetic strength is required to induce a strong enough attractive force to balance the electrostatic separation so that CNCs can be assembled into ordered arrays. On the other hand, the additional cleaning cycles significantly expand the range of wavelengths that the diffraction peak can be magnetically tuned over. For example, the diffraction maximum can be effectively tuned between 450 and 500 nm after a single water cleaning cycle with the sample−magnet distance in the range 2.6−3.5 cm, while the same sample after the fifth round of cleaning shows diffraction peaks tunable from 450 to 780 nm for the sample−magnet distance changing from 1.8 to 2.7 cm.

The diffracted intensity increases monotonically in the first three cleaning cycles, and then it fades slightly in further washing processes. The optimal assembly condition after three times of water cleaning favors the long-range order of the CNC arrays and therefore the strong diffractions. When the electrostatic repulsion is further enhanced by additional cleaning, more intense magnetic fields are required to induce a strong enough magnetic attractive force to balance the electrostatic force. This can be experimentally achieved by moving the magnet closer to the sample. However, when the magnet−sample distance is smaller than 2.3 cm, the gradient of the magnetic field increases dramatically (inset in Figure 4b) so that the magnetic packing force ($F_m = \nabla(\mu B)$) starts to affect the assembly behavior of the CNCs. The packing force applies to every particle and attracts them toward the maximum of local magnetic gradient, thus disturbing the long-range order inside the CNC chains and diminishing the diffracted intensity. Moving the magnet even closer further increases the magnetic packing force, eventually destabilizing the dispersion and precipitating CNCs on the glass vial wall.

We have also systematically studied the influence of the electrolyte concentration on the optical response of the samples. Figure 6 summarizes the change in position and intensity of the diffraction peak for a cleaned CNC solution with varying NaCl concentrations (0−1 mM) for nine sample−magnet distances. Due to screening by the counterions present in a double layer around each particle, the magnitude of the electrostatic repulsive force decreases strongly with increasing concentration of stray electrolytes.[49−51] As a result, the diffraction peak blue-shifts. From Figure 6a, it is obvious that the peak shift is more significant at lower ionic strength for the same amount of variation in the magnetic field. Data on the diffracted intensity as a function of electrolyte concentration and magnet−sample distance are displayed in Figure 6b, illustrating that maximum diffraction intensity is achieved at an optimal balance between magnetic and electrostatic interactions. For a strong magnetic field (magnet−sample distance 2.3−2.7 cm), bright diffractions are achievable at a low electrolyte concentration ($C_{NaCl} = 0$), where the induced magnetic attraction is strong enough to counter electrostatic repulsion. Increasing the electrolyte concentration reduces interparticle electrostatic repulsion. Apparently, as the repulsive forces weaken, positional order weakens monotonically, leading to the steady decrease in the diffraction intensity with increased electrolyte concentration. For samples in a weaker magnetic field (magnet−sample distance 2.8 to 3.1 cm), the induced magnetic attractive force has the appropriate magnitude

(49) Derjaguin, B. V.; Landau, L. *Acta Physicochim. URSS* **1941**, *14*, 633−662.
(50) Verwey, E. J. W.; Overbeek, J. T. G. *Theory of Stability of Lyophobic Colloids*; Elsevier: Amsterdam, 1948.
(51) Crocker, J. C.; Grier, D. G. *Phys. Rev. Lett.* **1994**, *73*, 352−355.

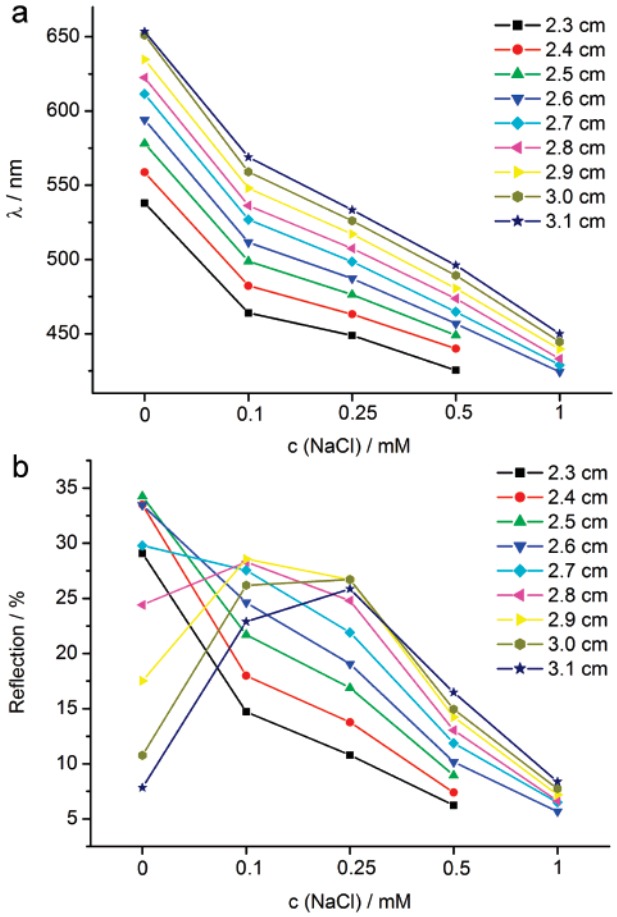

Figure 6. Influence of additional electrolyte NaCl on the (a) wavelength and (b) intensity of the diffraction peaks.

to counter the reduced electrostatic force achieved at a certain, nonzero electrolyte concentration. As a result, the diffraction intensity in this case first increases with the addition of NaCl, reaches a maximum at $C_{NaCl} = 0.1-0.25$ mM, and eventually decreases at even higher NaCl concentrations where the electrostatic force becomes too weak to produce optimal ordering within chains of particles.

Size Dependence of the Tuning Range of Diffractions. The range of the diffraction wavelengths that can be tuned by the external magnetic field has been found to relate to the mean size of the Fe_3O_4 CNCs. Figure 7 shows the TEM images and reflection spectra of four representative samples with sizes of $\sim 91 \pm 11$, 108 ± 23, 130 ± 20, and 180 ± 26 nm as determined by measuring the size of $\sim$200 clusters in TEM images for each sample. There is a consistent correlation between average particle size and the wavelength of the diffraction peaks. Comparatively speaking, smaller CNCs form ordered structures only under stronger magnetic fields with the formed structures preferably diffracting blue light (Figure 7a). Larger clusters diffract red light in a relatively weak magnetic field, and the ordered structures become unstable when the magnetic field strength is increased (Figure 7d). Medium-size clusters ($\sim$100−150 nm) self-assemble into stable ordered structures in both weak and strong magnetic fields, making their diffractions tunable from blue to green, yellow, and red (Figure 7b and c). The size-dependent optical property can be attributed to the strong size-dependent magnetic moments of the CNC particles. As reported previously, the saturated magnetic moments of individual particles increases dramatically when the particle size changes from a few nanometers to $\sim$180 nm.[41] When CNCs are small, they need a strong external field and

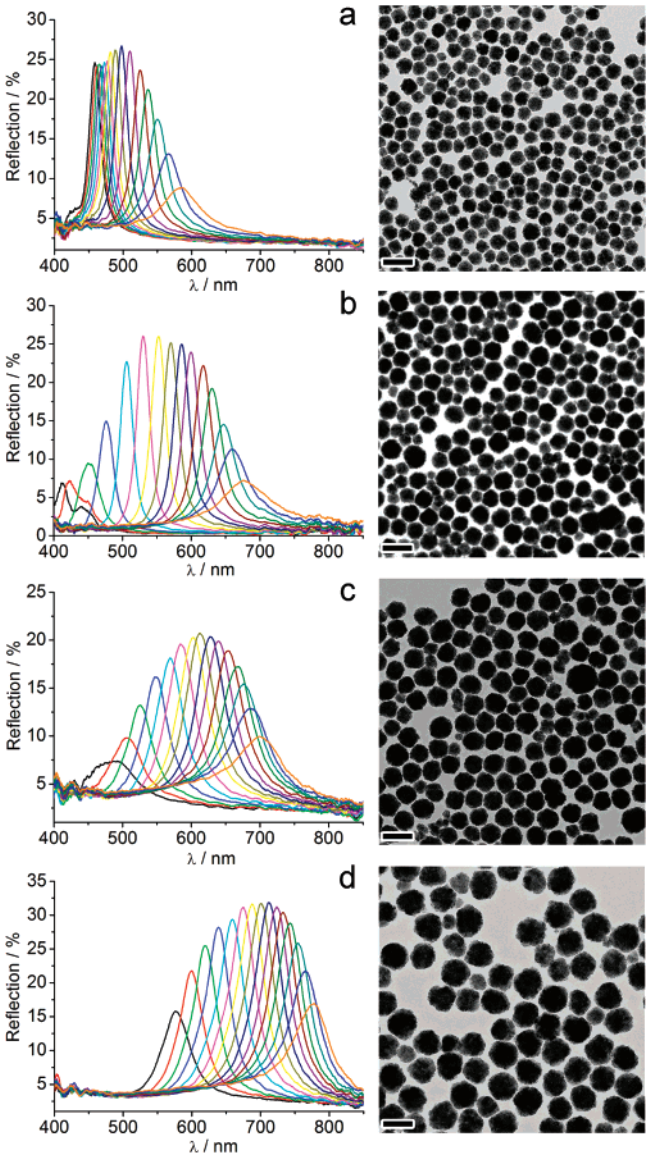

Figure 7. Dependence of the tuning range for diffraction on particle size. The average diameter of Fe_3O_4 CNCs in (a−d) is estimated to be 91, 108, 130, 180 nm, respectively, from TEM images. All scale bars correspond to 200 nm. For each sample, the diffraction peak blue-shifts as the magnet−sample distance decreases from (a) 2.6 to 1.2 cm, (b) 3.2 to 1.8 cm, (c) 3.5 to 2.1 cm, and (d) 3.7 to 2.3 cm.

short interparticle distances to induce enough magnetic attractive force for assembly into ordered structures. When CNCs are large, strong attraction can be induced even under relatively weak external fields so that the particles can be easily assembled at relatively large interparticle separations. The high value of magnetic moment of large CNCs also significantly increases the magnetic packing force, which makes the ordered structure unstable in strong external magnetic fields.

Interestingly, the tuning range of the diffraction wavelength can be broadened by mixing CNCs with two different sizes. Although a broad particle size distribution severely deteriorates the optical response of the CNCs, a mixture of two monodisperse colloids with different average particle sizes still displays reasonably strong diffraction. Figure 8 shows the reflections of two samples with sizes of $\sim$75 and 116 nm and their 1:1 (in mass ratio) mixture in response to external magnetic fields, with the spectra recorded at the same magnet−sample distance coded in the same color. The corresponding TEM images are also included

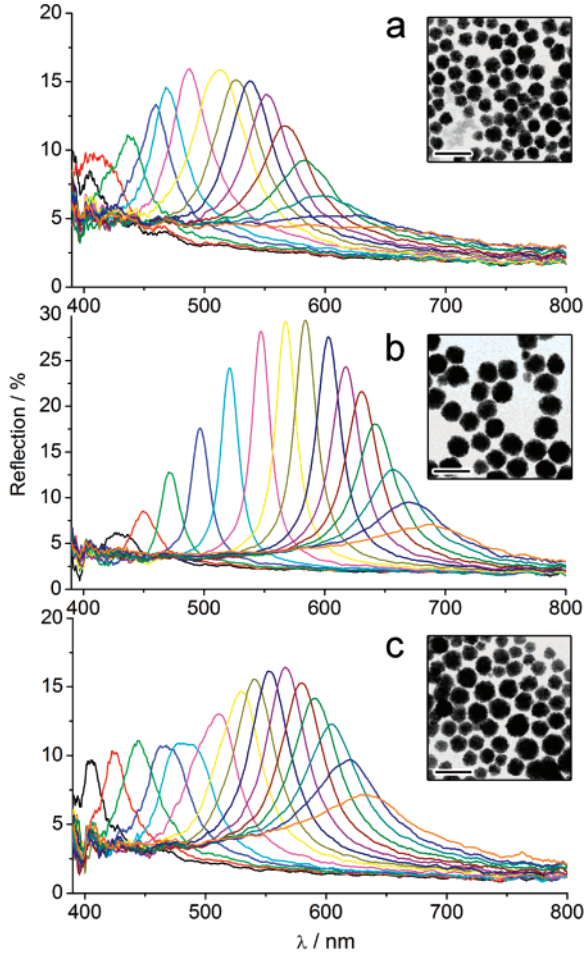

Figure 8. Reflection spectra of (a) ~75 nm and (b) ~116 nm Fe_3O_4 CNCs and (c) their 1:1 (in mass ratio) mixture in response to external magnetic fields. Since (a) and (b) are similar in size, the mixture shows slight broadening of the diffraction tuning range. In all cases, diffraction peaks blue-shift as the magnet−sample distance decreases from 3.3 to 1.9 cm. The scale bars correspond to 200 nm.

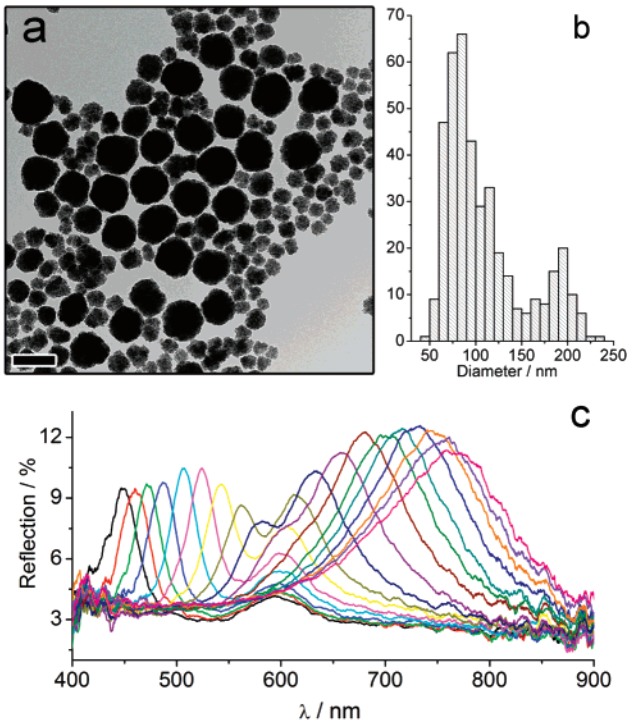

Figure 9. Broadening of the diffraction tuning range by mixing two Fe_3O_4 CNC samples with a large difference in size. (a and b) Representative TEM image and corresponding size distribution of the mixture of ~90 nm and 190 nm CNCs (in a mass ratio of 1:2.1). The scale bar corresponds to 200 nm. (c) Reflection spectra of the mixture as the magnet−sample distance decreases from 3.4 to 1.8 cm.

as insets. Since the average sizes of the original samples are close to each other, their mixture displays single diffraction peaks in a magnetic field with fixed strength. The tuning range has been slightly broadened in comparison to those of the original samples. Apparently, ordered structures still form in a solution of CNCs with mixed sizes under external fields. Careful comparison of the spectra for the samples before and after mixing reveals two interesting features that can help to elucidate the assembled structures in the mixed solutions. First, each diffraction peak of the mixture at a specific field strength is positioned between the peaks of the two original samples. However, the former is not the result of a simple overlay of the latter two, suggesting that the average interparticle distance of the CNCs in the mixture has a value between those in the original samples. Second, the overall diffracted intensity is lower than those of the original samples, especially in the longer wavelength, indicating considerable disruption to long-range order resulting from the mixing of particle populations of two different sizes.

By mixing two samples with a large size difference, we have been able to further increase the tuning range of the diffractions. Figure 9a and b shows the TEM image and size distribution of a sample obtained by mixing ~90 and 190 nm clusters in a mass ratio of 1:2.1. The reflection spectra of the mixture are displayed in Figure 9c. Different from the previous case, the reflection spectra of the mixture seem to be the simple overlay of those of the two original samples. In a weak magnetic field, the optical response appears to result from the ordering of large particles and the solution displays red diffractions, while in a strong field the diffraction is mainly due to the ordering of small particles and the solution shows blue color. In a magnetic field of intermediate strength, the large and small particles appear to assemble independently so that the reflection spectra are split into two peaks.

The Concentration Effect. Unlike traditional three-dimensional photonic crystals which are assembled from highly concentrated colloids, the system described in this work displays stronger diffraction at optimally diluted conditions. Figure 10 shows the reflection spectra of a sample in five different concentrations by dilution from 33.6 to 2.1 mg/mL. For each concentration, reflection spectra obtained at the same sample−magnet distance were plotted in the same color. Overall, the system shows a trend of red-shifting of the diffraction peaks upon dilution. There are very small changes in the peak positions and widths when the system is diluted from high concentrations (33.6 mg/mL) to the medium value (8.4 mg/mL), suggesting that a high particle concentration does not significantly change the assembly behavior of the CNCs (Figure 10a−c). The magnetic fields that are required to initiate the ordering of the CNC particles are also similar in strength for these three concentrations. The intensity of the diffractions, on the other hand, is lower at higher concentrations, probably due to the increased absorption at a higher loading of Fe_3O_4 materials. Further dilution of the system from 8.4 to 4.2 and eventually to 2.1 mg/mL greatly red-shifts the diffraction peaks, while the peak intensities remain almost unchanged. Interestingly, the strengths of the magnetic fields have to be increased to organize the particles in diluted solutions to display strong diffractions.

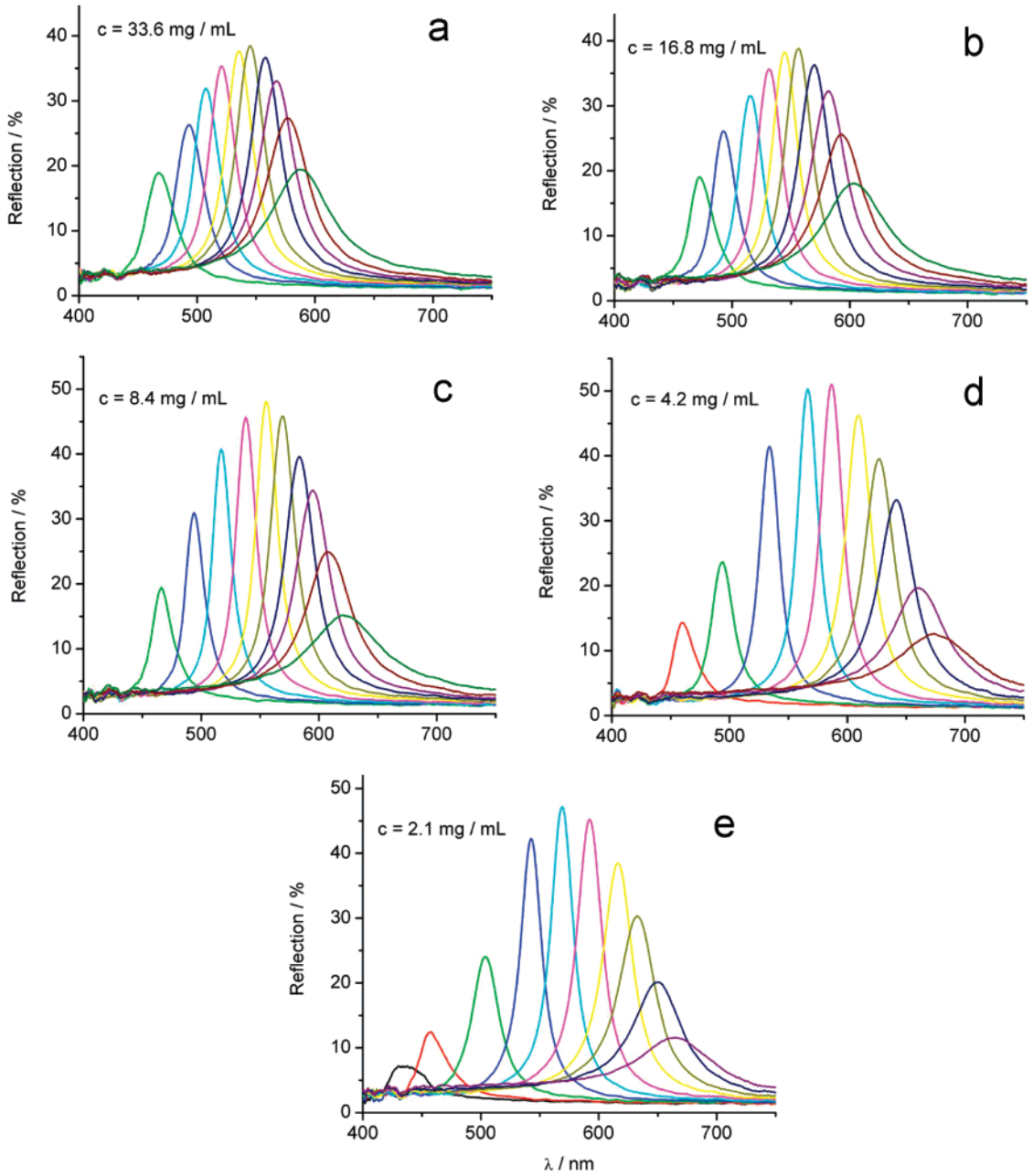

Figure 10. Influence of CNC concentration on the diffraction tuning range. Diffraction peaks blue-shift as the magnet−sample distance decreases from (a−c) 3.0 to 2.1 cm, (d) 2.9 to 2.0 cm, and (e) 2.8 to 1.9 cm. Peaks obtained at a specific magnet−sample distance were assigned the same color.

It is therefore believed that the electrostatic repulsive interactions are enhanced upon dilution, probably because such dilution also decreases the concentration of electrolytes. We found that a concentration in the range 4.2−8.4 mg/mL was optimal in terms of diffraction intensity and tuning range. If the solution is diluted to a concentration below 1.0 mg/mL, almost no visible diffractions can be observed.

Fast Response to Modulated Magnetic Fields. The Fe_3O_4 colloidal solutions possess a fast optical response to the external magnetic field, a feature critical for applications. To characterize the response time, we recorded the change of reflections in the presence of a periodically on−off magnetic field with a controllable switching frequency. Figure 11a shows successive reflection spectra recorded for a solution containing 130 nm Fe_3O_4 CNCs in response to a 0.5 Hz periodic magnetic field. The green diffraction at ∼535 nm clearly switches on and off with the same frequency as the external field. The reflected intensity continues to increase (albeit at a sharply decreasing rate) through the "on" phase of the cycle; however, no significant sharpening or shift of the diffraction peak is visible during that phase. A reasonable interpretation is that smaller structures with a distribution of interparticle spacings mimicking the equilibrium distribution form quite fast (in a period shorter than the integration time of our spectrometer, 200 ms). On the other hand, the growth, alignment, and merging of these ordered chains into longer ones appears to proceed over a longer time (on the scale of seconds). Similar modulation can be obtained for 70 and 180 nm Fe_3O_4 CNCs, which periodically diffract blue and red light at ∼470 and ∼654 nm, respectively.

Figure 11b−d shows the intensity change of the peaks at 470, 535, and 654 nm for the three samples in a faster, 1 Hz alternating magnetic field. One can clearly see that the peak intensity increases gradually during the "on" stage of the magnetic field, indicating continuous improvement of the long-range order of the CNCs.

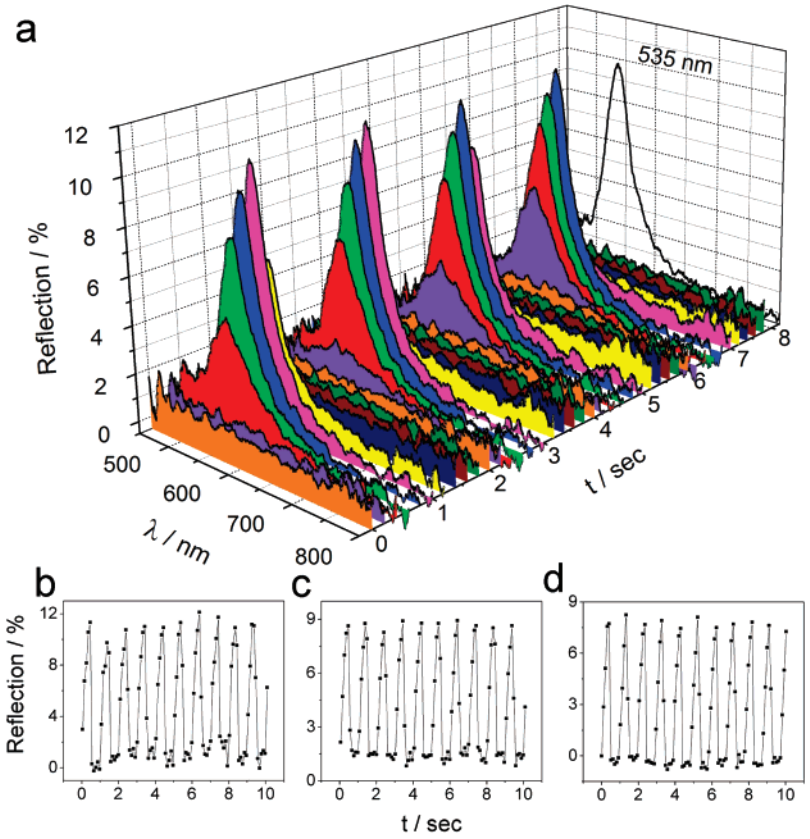

Figure 11. (a) Modulated diffractions of a 130 nm CNC solution in a 0.5 Hz periodic magnetic field, with a spectra integration time of 200 ms. (b−d) Variation of the diffraction peak intensity at (b) 470 nm, (c) 535 nm, and (d) 654 nm for 70, 130, and 180 nm colloidal photonic crystals in a 1 Hz periodic magnetic field, with a spectra integration time of 100 ms.

The diffraction peak disappears completely within 100−200 ms after the magnetic field is off, which is much faster than the development of perfect translational order under a magnetic field. Carefully comparing the intensity profile of the diffraction peaks of three samples with the same frequency, one can find that the "blue" sample of smaller CNCs with a diffraction peak at 470 nm takes less time than the "red" sample of larger CNCs to reach maximum intensity, probably due to the smaller size and higher mobility.

On the basis of visual observations, we believe the colloidal solution confined in a glass capillary may respond to the external magnetic field at even higher frequencies. However, no such measurements have been attempted at higher switching speed due to the limitation of the integration time of our charge-coupled device (CCD) detectors. The nucleation of an initial region with regular interparticle and interchain distances might be facilitated by the boundary conditions in a confined volume, suggesting the study of ordering kinetics in a range of confined volumes as an interesting area of research. On the other hand, the rapid switching rate of the described systems in response to external magnetic signals implies wide potential use in telecommunication and optoelectronic devices.

Conclusions

Superparamagnetic colloidal nanocrystal clusters of magnetite with highly charged surfaces have been assembled into ordered structures in solution under external magnetic fields. The ordering of the particles was achieved as the balanced interactions including the electrostatic forces and externally induced magnetic forces. Although the assembled structures are three-dimensional, long-range order is only achieved along the direction of the magnetic field with interparticle spacing comparable to the wavelength of visible light. As a result, the colloidal solutions show strongly diffraction in the visible spectrum in the direction of external magnetic fields. Since the interparticle spacing is determined by the relative strengths of electrostatic repulsions and magnetic attractions, the diffraction peaks can be tuned across the entire visible spectrum by simply changing the strength of the magnetic field. The concentration of stray electrolytes also has a strong effect on the optical response of the solution, as it changes the strength of the interparticle electrostatic repulsion. Other factors including the size, size distribution, and concentration of the colloids have also been examined to optimize the diffraction intensity and tuning range. With further demonstrations of their rapid, reversible, and fully tunable field-responsive photonic properties, we believe these materials represent a new platform for the fabrication of novel optoelectronic devices, sensors, and color displays.

Acknowledgment. Y.Y. thanks the University of California, Riverside for start-up funds and Dr. C. K. Erdonmez for helpful discussion. We thank Prof. W. P. Beyermann and Dr. M. Biasini for help with magnetic property measurements, Mr. C. D. Graham for fabricating the electromagnet system, and Dr. Bozhilov and Mr. McDaniel at the Central Facility for Advanced Microscopy and Microanalysis at UCR for assistance with TEM analysis.

LA7039493